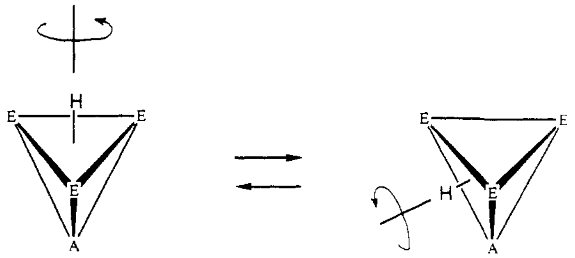

Figure 5. Representation of a mechanism that interchanges all carbonyl groups in the solid state for a face-capped tetrahedron.

as a twist mechanism is unlikely in the solid state for [HFe(CO)$_4$]$^-$. A hydride tunnelling mechanism appears to be more likely since it requires minimal movement of the carbonyl ligands.

A similar conclusion was reached from the study of HML$_4$ complexes in solution.[1-3] It was argued that for transition-metal complexes the Berry rotation applies to structures of rigorous square-pyramidal or trigonal-bipyramidal structure. On this basis then the hydride tunnelling mechanism is also more likely in the solid since the structure of the carbonyl hydride is distorted away from an ideal trigonal bipyramid.

Hydride tunnelling has also been proposed to occur in the closely related complexes H$_2$Fe(CO)$_4$[23] and H$_2$Fe(PR$_3$)$_4$.[24] For these distorted-octahedral complexes hydride tunnelling exchanges axial and equatorial carbonyl groups. In solution the barrier to hydride tunnelling for H$_2$Fe(CO)$_4$ was estimated to be 8.1 kcal mol^{-1}.[23] Axial-equatorial exchange is also rapid in solution for the anion, [HFe(CO)$_4$]$^-$; the average chemical shift observed in solution is 220.8 ppm at room temperature.[23] In the solid state the barrier for axial-equatorial exchange is 7.0 ± 0.7 kcal mol^{-1} for [NEt$_4$][HFe(CO)$_4$], significantly higher than the appearent solution value, and the isotropic chemical shift in the fast exchange limit is 221.6 ppm, in good agreement with the solution value.

Closer examination of the dynamic processes that may take place in the solid state suggests that, in addition to the hydride tunnelling, another motion is required to make the carbonyl environments truly equivalent. Since the anion in [PPN][HFe(CO)$_4$] lies on a general position the four carbonyl ligands are crystallographically unique. This suggests that either the resonances due to the three equatorial carbonyls in the anion are degenerate at low temperature or there is an additional motion that makes these groups magnetically equivalent. It is well established that chemically identical but crystallographically unique carbonyl ligands can show different resonances in the solid state.[25] If rotation about the 3-fold axis in the anion is fast in the solid state then all four carbonyls can in fact become equivalent in the solid state when hydride tunnelling and the 3-fold rotation are combined. This is shown schematically in Figure 5. Rotation about molecular 3-fold axes is established in (η^6-C$_6$H$_5$CH$_3$)Mo(CO)$_3$ and related metal carbonyls[19] as well as in Fe(CO)$_5$ (vide supra).

Acknowledgment. We thank Dr. Larry Sterna, Shell Development and Research Corporation, Houston, TX, for preliminary MAS spectra of [NEt$_4$][HFe(CO)$_4$]. We thank Tom Glass for assistance in constructing the NMR instrumentation; Ipin Guo helped in obtaining the spectra of [PPN][HFe(CO)$_4$]. Support of this work was provided by the Robert A. Welch Foundation (K.H.W.) and the National Science Foundation (B.E.H).

---

(23) Whitmire, K. H.; Lee, T. R. *J. Organomet. Chem.* **1985**, *282*, 95.

(24) Meakin, P.; Meutterties, E. L.; Jesson, J. P. *J. Am. Chem. Soc.* **1973**, *95*, 75.

(25) (a) Dorn, H. C.; Hanson, B. E.; Motell, E. *J. Organomet. Chem.* **1982**, *224*, 181. (b) Aime, S.; Botta, M.; Gobetto, R.; Osella, D. *Inorg. Chim. Acta.* **1988**, *146*, 151. (c) Walter, T. H.; Reven, L.; Oldfield, E. *J. Phys. Chem.* **1989**, *93*, 1320. (d) Hasselbring, L.; Lamb, H.; Dybowski, C.; Gates, B. C.; Rheingold, A. *Inorg. Chim. Acta* **1987**, *127*, 149.

Hydration Structure of Titanium(III) Ion. ESR and Electron Spin-Echo Study

Hiroto Tachikawa, Tsuneki Ichikawa,* and Hiroshi Yoshida

Contribution from the Faculty of Engineering, Hokkaido University, Sapporo 060, Japan.
Received May 2, 1989

Abstract: ESR, ENDOR, and electron spin-echo studies have been carried out for determining the hydration structure of the Ti^{3+} ion in the amorphous solid of a 2-propanol/D$_2$O mixture. It is found that the hydrated ion is in D_{3d} symmetry with the unpaired electron mainly in the d$_{z^2}$ orbital. Six water molecules coordinate to the central metal ion with the Ti^{3+}–O distance of about 2.2 Å to form an octahedron with a slight compression along the C_3 axis. Because of the strong repulsive interaction between the d$_{z^2}$ orbital and the n$_\pi$ orbitals of the coordinating D$_2$O molecules, the D–O–D planes are almost parallel to the C_3 axis. The angle between the C_3 axis and the Ti^{3+}–O bond is about 60°. The value of $g_\parallel$ is 1.994, but the value of $g_\perp$ is distributed around 1.896. The hydrated ion with lower $g_\perp$ value shows weaker isotropic hyperfine coupling with the coordinated water deuterons, which is well interpretted as due to the displacement of the D–O–D planes from the parallel configuration.

The trivalent titanium ion, Ti^{3+}, is one of the simplest paramagnetic metal ions and has been frequently cited as a good example for explaining crystal field or ligand field theory. However, ESR studies of the Ti^{3+} ion are rather few, probably because of its chemical instability. The ESR spectrum of the hydrated Ti^{3+} ion in cesium alum, CsTi(SO$_4$)$_2$·12H$_2$O, was measured below 8 K by Bijl,[1] who reported the $g_\parallel$ of 1.25 and $g_\perp$ of 1.14. Since the structure of the hydrated ion in the alum crystal was expected to be nearly regular octahedron,[2-4] the g anisotropy was explained as due to the splitting of the $^2T_{2g}$ state into the $^2A_{1g}$ state by a slight compression of the coordinated water molecules about the C_3 axis and by covalent bonding between the metal ion

---

(1) Bijl, D. *Proc. Phys. Soc.* (*London*) **1950**, *A63*, 405.

(2) Haussuhl, V. S. *Z. Kristallogr.* **1961**, *116*, 371.

(3) Lipson, H. *Proc. R. Soc. A* **1935**, *151*, 347.

(4) Lipson, H.; Beevers, C. A. *Proc. R. Soc. A* **1935**, *148*, 664.

0002-7863/90/1512-977$02.50/0

and the water molecules.[1,5] The chelated complex titanium tris(acetylacetonate) also gives an axially symmetric ESR spectrum.[6] Although the oxygen atoms of the chelated complex form nearly regular octahedron, the observed g factors, $g_{\parallel} = 2.00$ and $g_{\perp} = 1.93$, are much different from those of the hydrated ion in the alum crystal, which indicates that the axial field of the metal complex is very sensitive to the covalency between the metal ions and ligands. However, the relation between the axial field and the covalency has not been fully understood. The electronic spectrum of the hydrated Ti^{3+} ion in water appearing around 500 nm has also been known as a good example of crystal field splitting of degenerate d orbitals. However, as will be mentioned in the next paper, the ground and the excited electronic states of the hydrated Ti^{3+} ion have also not been fully understood.

One way to know the ground and excited electronic states is to analyze the ESR spectrum of the hydrated Ti^{3+} ion. Although the ESR spectrum of the hydrated Ti^{3+} ion in the alum crystal is known, it is not certain whether the hydration structure is the same in the crystal and in water, because the hydration structure in the crystal might be distorted by the interaction between the surrounding water molecules and ions. To measure the ESR spectrum of the hydrated Ti^{3+} in water is therefore necessary. However, the ESR spectrum is impossible to measure because of the fast paramagnetic relaxation rate. In the present paper ESR and electron spin-echo (ESE) modulation studies on the hydrated Ti^{3+} ion in the amorphous solid of a 2-propanol/D_2O mixture have been carried out for determining the structure of the hydrated Ti^{3+} ion in water and for clarifying the origin of the axial field. Since the amorphous solid has no long-range order, the Ti^{3+} ion in the amorphous solid is expected to maintain the same hydration structure in water.

Experimental Section

About 10^{-2} mol/dm^3 of Ti^{3+} in water containing 33 vol % of 2-propanol was transferred into a quartz tube and then frozen in liquid nitrogen immediately after the preparation of the solution. 2-Propanol was used for preventing the crystallization of the solution. For observing the ESE nuclear modulation from the coordinated water molecule, D_2O was used instead of H_2O because deuterons give much stronger modulation than protons. Deuterated 2-propanol (C_3D_7OH) was used for observing the ESE modulation from the nuclei located out of the first coordination sphere. A C_3H_7OH/H_2O mixture was used for observing the ENDOR spectrum of Ti^{3+}. The optical absorption spectra were recorded at 293 and 77 K on a Shimazu MPS-1000 spectrophotometer. The ESR and ENDOR spectra were measured at 77 and 12 K, respectively, on a Bruker X-band spectrometer. The ESE signals were recorded at 4.2 K on a home-built X-band ESE spectrometer[7] with the pulse width of 60 ns, which was wide enough for suppressing the nuclear modulation by protons. Two-pulse ESE signals were recorded as a function of the time interval between the first and the second microwave pulses, τ. The deuteron nuclear modulation observed on the ESR signal was analyzed for determining the hydration structure of the Ti^{3+} ion.

Data Analysis

The detailed theory of ESE modulation resulting from nuclear hyperfine and quadrupole interactions with a magnetic nucleus has been given in a previous literature citation,[8] so we only show the final result.[9] The ESE signal as a function of the time interval τ between the first and the second microwave pulses is given by the product of a monotonous decay function $D(\tau)$ and the theoretical modulation function for the ith nuclear spin, $E_i(\tau)$, as

$$E(\tau) = D(\tau) \prod_{i=1}^{M} E_i(\tau) \tag{1}$$

where M is the total number of nuclear spins surrounding the electron spin, $E_i(\tau)$ has the form

$$\begin{aligned}
E_i(\tau) = {} & 1 - (\omega_1 B/\omega_\alpha\omega_\beta)^2\{I(I+1)/3\} \times \\
& [\cos(\omega_\alpha\tau - \omega_\beta\tau)C_1(\gamma_\alpha\tau - \gamma_\beta\tau) + \cos(\omega_\alpha\tau + \omega_\beta\tau)C_1(\gamma_\alpha\tau + \\
& \gamma_\beta\tau) - 2\cos(\omega_\alpha\tau)C_1(\gamma_\alpha\tau) - 2\cos(\omega_\beta\tau)C_1(\gamma_\beta\tau) + 2] + \\
& (\omega_1/\omega_\alpha\omega_\beta)^3 B(B\gamma + 2A\mu_1 - B\mu_2) \times \\
& [2\sin(\omega_\alpha\tau)S_1(\gamma_\alpha\tau) + 2\sin(\omega_\beta\tau)S_1(\gamma_\beta\tau) - \sin(\omega_\alpha\tau + \\
& \omega_\beta\tau)S_1(\gamma_\alpha\tau + \gamma_\beta\tau) + \sin(\omega_\alpha\tau - \omega_\beta\tau)S_1(\gamma_\alpha\tau - \gamma_\beta\tau)] + \\
& (\omega_1 B/\omega_\alpha\omega_\beta)^4\{I(I+1)(2I-1)(2I+3)/240\} \times \\
& [12\cos(\omega_\alpha\tau - \omega_\beta\tau)C_2(\gamma_\alpha\tau - \gamma_\beta\tau) + 12\cos(\omega_\alpha\tau + \\
& \omega_\beta\tau)C_2(\gamma_\alpha\tau + \gamma_\beta\tau) - 24\cos(\omega_\alpha\tau)C_2(\gamma_\alpha\tau) - \\
& 24\cos(\omega_\beta\tau)C_2(\gamma_\beta\tau) + \cos(2\omega_\alpha\tau + 2\omega_\beta\tau)C_3(4\gamma_\alpha\tau + 4\gamma_\beta\tau) + \\
& \cos(2\omega_\alpha\tau - 2\omega_\beta\tau)C_3(4\gamma_\alpha\tau - 4\gamma_\beta\tau) + \\
& 6\cos(2\omega_\alpha\tau)C_3(4\gamma_\alpha\tau) + 6\cos(2\omega_\beta\tau)C_3(4\gamma_\beta\tau) + \\
& 4\cos(\omega_\alpha\tau + \omega_\beta\tau)\cos(\gamma_\alpha\tau - \gamma_\beta\tau)C_3(2\gamma_\alpha\tau + 2\gamma_\beta\tau) + \\
& 4\cos(\omega_\alpha\tau - \omega_\beta\tau)\cos(\gamma_\alpha\tau + \gamma_\beta\tau)C_3(2\gamma_\alpha\tau - 2\gamma_\beta\tau) - \\
& 4\cos(2\omega_\alpha\tau + \omega_\beta\tau)\cos(\gamma_\beta\tau)C_3(4\gamma_\alpha\tau + \\
& 2\gamma_\beta\tau) - 4\cos(2\omega_\alpha\tau - \omega_\beta\tau)\cos(\gamma_\beta\tau)C_3(4\gamma_\alpha\tau - 2\gamma_\beta\tau) - \\
& 4\cos(\omega_\alpha\tau + 2\omega_\beta\tau)\cos(\gamma_\alpha\tau)C_3(2\gamma_\alpha\tau + 4\gamma_\beta\tau) - 4\cos(\omega_\alpha\tau - \\
& 2\omega_\beta\tau)\cos(\gamma_\alpha\tau)C_3(2\gamma_\alpha\tau - 4\gamma_\beta\tau) + 18]
\end{aligned} \tag{2}$$

where

$$A = (1/\hbar r^3)gg_N\beta\beta_N(3\cos^2\theta - 1) + 2\pi a, \quad B = (3/\hbar r^3)gg_N\beta\beta_N \sin\theta\cos\theta$$

$$\omega_1 = g_N\beta_N H/\hbar, \quad \gamma = [3e^2qQ/\{8I(2I-1)\hbar\}](3\cos^2\theta' - 1) = \gamma'(3\cos^2\theta' - 1)$$

$$\omega_{\alpha,\beta} = \{(\omega_1 \mp A/2)^2 + B^2/4)\}^{1/2}$$

$$\gamma_{\alpha,\beta} = \gamma'[3\{(\omega_1 \mp A/2)\cos\theta \mp (B/2)\sin\theta\cos(\phi' - \phi)\}/\omega_{\alpha,\beta}{}^2 - 1]$$

$$\mu_1 = \gamma'\sin\theta'\cos\theta'\cos(\phi' - \phi), \quad \mu_2 = (\gamma'/2)\sin^2\theta'\cos(2\phi' - 2\phi)$$

$$C_1(x) = [3/\{2I(I+1)(2I+1)\}]\sum_{m=-I}^{I}\{I(I+1) - m(m+1)\}\cos\{(2m+1)x\}$$

$$S_1(x) = \{1/(2I+1)\}\sum_{m=-I}^{I}\{I(I+1) - m(m+1)\}(2m+1)\sin\{(2m+1)x\}$$

$$C_2(x) = [15/\{2I(I+1)(2I+1)(2I-1)(2I+3)\}]\sum_{m=-I}^{I}\{I(I+1) - m(m+1)\}\{I(I+1) - (m^2+m+1)\}\cos\{(2m+1)x\}$$

$$C_3(x) = [15/\{2I(I+1)(2I+1)(2I-1)(2I+3)\}]\sum_{m=-I}^{I}\{I(I+1) - m(m+1)\}\{I(I+1) - m(m-1)\}\cos(mx) \tag{3}$$

and θ, ϕ are the polar and azimuthal angles of the vector r joining an unpaired electron and the interacting ith nucleus with the nuclear spin I, the isotropic hyperfine coupling constant a, and the quadrupole frequency e^2qQ/h with respect to z as polar axis parallel to the external magnetic field H, and θ', ϕ' are the polar and azimuthal angles of the direction of the quadrupole moment with respect to z. The other quantities have their usual meanings.

The monotonous decay function was approximated by

$$D(\tau) = \exp(d_0 + d_1\tau^{1/2} + d_2\tau + d_3\tau^2) \tag{4}$$

where the adjustable parameters d_i can be determined from the observed ESE signal by a least-squares method.[10]

Equation 1 can be treated more easily by dividing the interacting magnetic nuclei into two groups: one is the nuclei in the first

---

(5) Abragam, A.; Bleaney, B. *In Electron Paramagnetic Resonance of Transition Metal Ions*; Oxford University Press: London, 1970; p 417.

(6) Jarrett, H. S. *J. Chem. Phys.* **1957**, *27*, 1298.

(7) Ichikawa, T. *J. Magn. Reson.* **1986**, *70*, 280.

(8) Ichikawa, T. *J. Chem. Phys.* **1985**, *83*, 3790.

(9) There are several typographical errors in eqs. 10, 30, and 31 of ref 8. Equation 10 should be replaced by $\omega_{\beta,\alpha} = \{(\omega_1 \pm A/2)^2 + B^2/4\}^{1/2}$. Equations 30 and 31 should also be replaced by eqs 2 and 3 of the present paper.

(10) Ichikawa, T.; Miki, H.; Yoshida, H. *J. Phys. Chem.* **1985**, *89*, 1211.

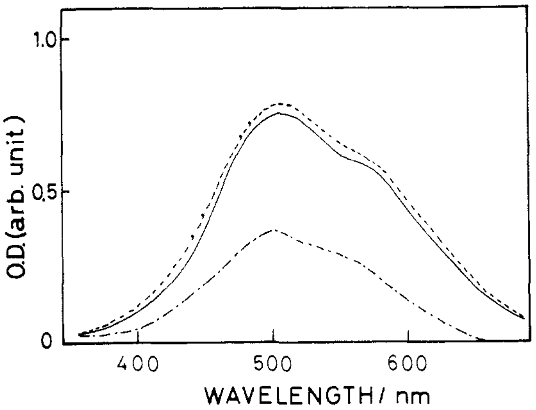

Figure 1. Optical absorption spectra of the Ti^{3+} ion in H_2O (—) and the 2-propanol/H_2O mixture (- - -) at 290 K and in the amorphous solid of the 2-propanol/D_2O mixture at 77 K (-·-).

coordination sphere and the other is those out of the first coordination sphere giving the nuclear modulation of $E_{\text{oui}}(\tau)$. Equation 1 is then expressed as

$$E(\tau) = D(\tau)E_{\text{oui}}(\tau)\prod_{i=1}^{N}E_i(\tau) \qquad (5)$$

where N is the total number of magnetic nuclei in the first coordination sphere. The function $E_{\text{oui}}(\tau)$ will be experimentally determined by measuring the ESE modulation from the nuclei located out of the first coordination sphere. If the paramagnetic species shows an axially symmetric ESR spectrum, which is the case for the hydrated Ti^{3+} ion, eq 5 is angular averaged as

$$E(\tau) = D(\tau)E_{\text{oui}}(\tau)\int_0^{2\pi}(1/2\pi)\prod_{i=1}^{N}E_i(\tau)\,d\xi = D(\tau)E_{\text{oui}}(\tau)E_{\text{ih}}(\tau) \qquad (6)$$

where ξ is the polar angle of the external magnetic field with respect to the symmetry axis of the paramagnetic species.

The following assumptions were made for analyzing the ESE modulation signals from the hydrated Ti^{3+} ion.

(1) The Ti^{3+} ion is coordinated by six water molecules. This assumption might be plausible because a coordination number of other than six is not known.

(2) The molecular structure of the coordinated D_2O is the same as that of Ni^{2+}-coordinated D_2O with the O–D distance of 1.09 Å and the D–O–D angle of approximately 104.5°,[11] and the molecular dipole of D_2O is oriented toward the central Ti^{3+} ion.[12,13]

(3) The unpaired electron is located at the center of the Ti^{3+} ion, so that the distance between the unpaired electron and the deuteron is given by

$$r = \{R^2 + 1.09^2 + 2(1.09)R\cos(104.5°/2)\}^{1/2}/\text{Å} \qquad (7)$$

where R is the distance between the coordinated oxygen and the central Ti^{3+} ion in angstroms.

(4) The quadrupole tensor for the coordinated D_2O is the same as that for free D_2O. That is, the principal axis of the tensor directs along the O–D bond and the value of e^2Qq_{zz}/h is 0.2 MHz.[14]

For determining the best geometrical parameters for the hydrated ion, the observed ESE signal of the hydrated Ti^{3+} ion in the C_3H_7OH/D_2O mixture was compared with the theoretical signal by a least-squares method as

$$\text{ERROR} = (1/n)\sum_{k=1}^{n}[E_{\text{obs}}(\tau_k) - D(\tau_k)E_{\text{oui}}(\tau_k)\{E_{\text{ih}}(\tau_k)\}^{\rho''}]^2 \qquad (8)$$

where $E_{\text{obs}}(\tau_k)$ is the observed ESE intensity at $\tau = \tau_k$ and ρ'' is the atomic ratio of O–D deuterons defined by $\rho'' = [\text{O–D}]/([\text{O–D}] + [\text{O–H}])$. The exponent ρ'' (=0.94) was added in eq 8 because a part of the O–D deuterons of the water molecules was replaced by O–H protons of 2-propanol molecules.

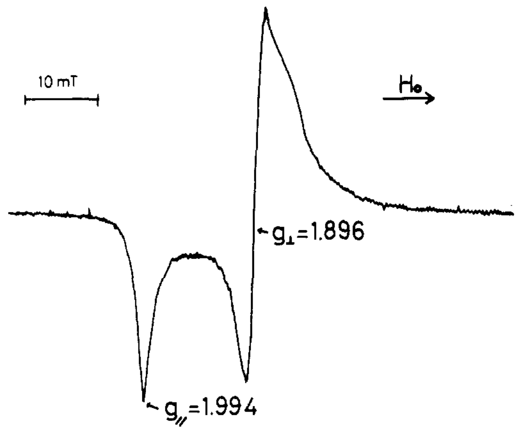

Figure 2. ESR spectrum of the hydrated Ti^{3+} ion in the 2-propanol/D_2O mixture at 77 K.

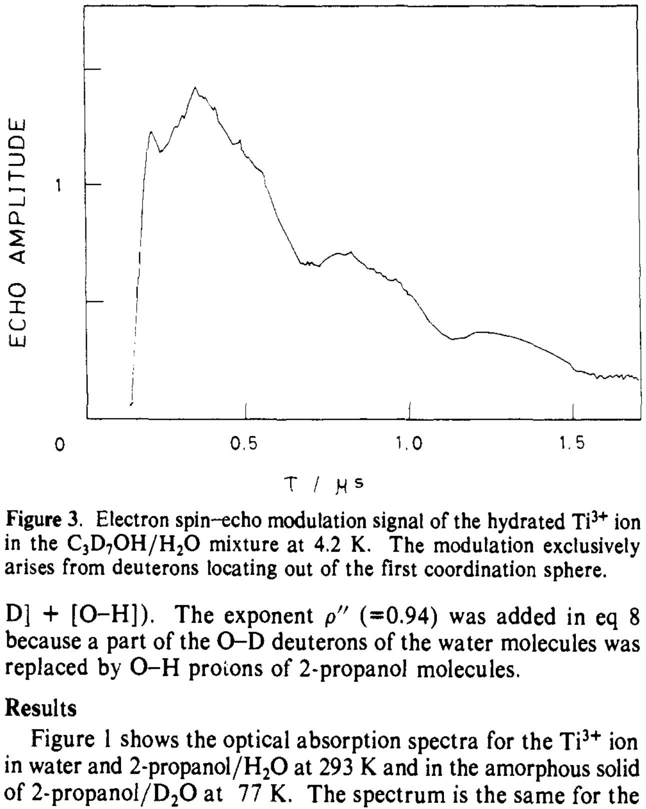

Figure 3. Electron spin–echo modulation signal of the hydrated Ti^{3+} ion in the C_3D_7OH/H_2O mixture at 4.2 K. The modulation exclusively arises from deuterons locating out of the first coordination sphere.

Results

Figure 1 shows the optical absorption spectra for the Ti^{3+} ion in water and 2-propanol/H_2O at 293 K and in the amorphous solid of 2-propanol/D_2O at 77 K. The spectrum is the same for the three solvents, which indicates that the Ti^{3+} ion is coordinated only by water molecules even though 2-propanol is added to the solvent and the hydration structure is the same in these solvents.

As is shown in Figure 2, the hydrated ion at 77 K gives an axially symmetric ESR spectrum with $g_{\parallel} = 1.994$ and $g_{\perp} = 1.896$. The value of $g_{\parallel}$ close to the g factor of a free electron implies that the hydrated ion possesses D_{3d} symmetry and the unpaired electron is mainly in the a_{1g} or, more simply, the d_{z^2} orbital of the Ti^{3+} ion. Although the shape of the spectrum is close to an ideal axially symmetric spectrum near the $g_{\parallel}$ position, it is much broader near the $g_{\perp}$ position. The spectrum extends up to 390 mT, which corresponds to $g_{\perp} = 1.687$. The broadness of the spectrum indicates that the $g_{\perp}$ factor is changed ion by ion because of the difference of the hydration structure.

Since 2-propanol is located out of the first coordination sphere, the function $E_{\text{oui}}(\tau)$ for the C_3H_7OH/D_2O mixture is determined from the ESE modulation for the C_3D_7OH/H_2O mixture, $E'_{\text{oui}}(\tau)$, as

$$E_{\text{out}}(\tau) = [E'_{\text{out}}(\tau)]^{\rho/\rho'} \qquad (9)$$

where ρ and ρ' are the number density of deuterons in the C_3H_7OH/D_2O and C_3D_7OH/H_2O mixtures, respectively. The value of ρ/ρ' was estimated to be 2.39. An example of the ob-

---

(11) Soper, A. K.; Nelson, G. W.; Enderby, J. E.; Howe, R. A. *J. Phys. C* **1977**, *10*, 1793.

(12) Bacon, G. E.; Gardner, W. E. *Proc. Roy. Soc. A* **1958**, *246*, 78.

(13) Caminiti, R.; Licheri, G.; Piccaluga, G.; Pinna, G. *J. Chem. Phys.* **1978**, *69*, 1.

(14) Iwasaki, M.; Toriyama, K. *J. Chem. Phys.* **1985**, *82*, 5415.

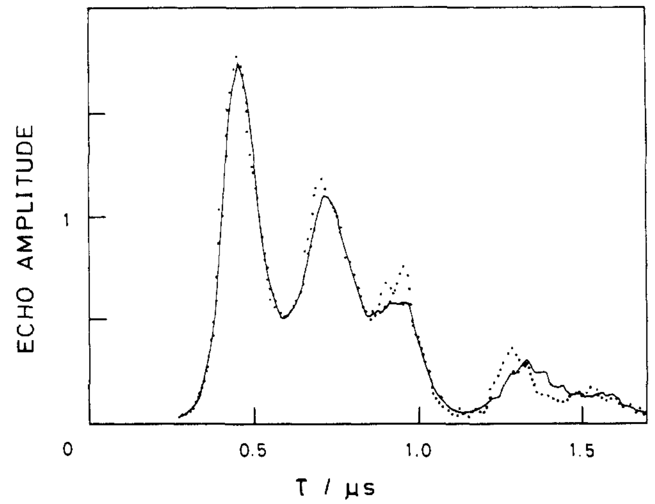

Figure 4. Electron spin-echo modulation signal of the hydrated Ti^{3+} ion in the C_3H_7OH/D_2O mixture at 4.2 K. The solid line shows the signal recorded at the magnetic field of 328 mT corresponding to $g_\parallel = 2.000$. The dotted line shows the best simulation obtained by using the parameters $e^2qQ_{zz}/h = 0.2$ MHz, $R = 2.2$ Å, $N = 12$, $\zeta = 60°$, $\psi = 0°$, $\xi = 0°$, and $a = 0.85$ MHz.

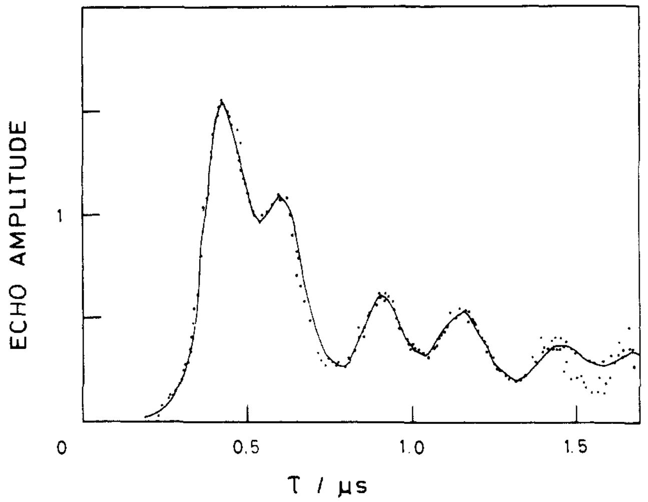

Figure 5. Electron spin-echo modulation signal of the hydrated Ti^{3+} ion in the C_3H_7OH/D_2O mixture at 4.2 K. The solid line shows the signal recorded at the magnetic field of 370 mT corresponding to $g_\perp = 1.778$. The dotted line shows the best simulation obtained by using the parameters $e^2qQ_{zz}/h = 0.2$ MHz, $R = 2.2$ Å, $N = 12$, $\zeta = 60°$, $\psi = 0°$, $\xi = 90°$, and $a = 0.45$ Mz.

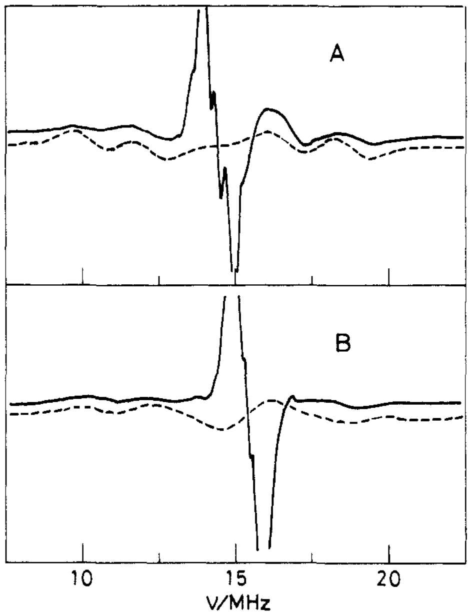

Figure 6. First-derivative ENDOR spectra of the hydrated Ti^{3+} ion in the C_3H_7OH/H_2O mixture at 12 K. The solid lines show the spectra recorded at the magnetic fields of (A) 338 mT and (B) 360 mT corresponding to $g_\parallel = 1.996$ and $g_\perp = 1.872$, respectively. The broken lines show the simulated spectra obtained by assuming a Gaussian line shape of $\exp(-\nu^2/w^2)$ with $w = 2$ MHz and by using the parameters $R = 2.2$ Å, $N = 12$, $\zeta = 60°$, $\psi = 0°$, (A) $\xi = 0°$, $a = 7$ MHz, and (B) $\xi = 90°$, $a = 5$ MHz.

served $E'_{\rm out}(\tau)$ is shown in Figure 3. Only a very weak nuclear modulation due to distant deutrons is observed, which confirms that the Ti^{3+} ion is not coordinated by 2-propanol molecules.

Figure 4 shows the ESE signal of the hydrated ion in the C_3H_7OH/D_2O mixture recorded at 4.2 K by fixing the magnetic field at 329 mT corresponding to the $g_\parallel$ value of 2.000. Since the ESR spectrum of the hydrated ion near the $g_\parallel$ region is close to an ideal axially symmetric spectrum, the observed ESE signal exclusively arises from the hydrated ion with the symmetry axis parallel to the external magnetic field. The ESE modulation is composed of single and double deuteron Larmor frequencies. The amplitude of the double-frequency component is much stronger than those for other hydrated transition-metal ions such as Cu^{2+} and Mn^{2+},[10] which suggests that the D_2O deuterons coordinated to Ti^{3+} have rather high isotropic hyperfine coupling constants.

Since the hydrated ion is in D_{3d} symmetry, the location of the deuterons on the coordinated water molecules can be expressed by three parameters: R, the distance between the Ti^{3+} ion and the coordinated oxygen atom; ζ, the angle between the C_3 axis and the Ti^{3+}–O bond, and ψ, the angle between the C_3 axis–Ti^{3+}–O plane and the D–O–D plane. The observed ESE signal was simulated as a function of the above three parameters and the isotropic hyperfine coupling constant a. The simulated modulation pattern was very sensitive to ζ and a, and the best fit of the observed signals was obtained at $\zeta = 60°$ and $a = 0.85$ MHz. The modulation pattern was less sensitive to R and ψ. The best fit was obtained at $R = 2.2 \pm 0.5$ Å and $\psi = 0 \pm 15°$. The ESE signal calculated by using $R = 2.2$ Å and $\psi = 0°$ is shown in Figure 4 with a dotted line.

Since the value of $g_\perp$ is changed ion by ion, the ESE signal at $g_\perp = 1.896$ does not exclusively arise from the hydrated ions with the symmetry axis perpendicular to the external field. The external field for the ESE measurement was therefore shifted to the higher field of 370 mT for increasing the purity of the $g_\perp$ component. As is shown in Figure 5, the ESE signal observed at 370 mT corresponding to $g_\perp = 1.778$ was simulated well by using the geometrical parameters for the $g_\parallel$ component and $a = 0.45$ MHz. However, the spectrum was not simulated well if $a = 0.85$ MHz was used for the calculation. The above result indicates that the hydrated ion with the lower a value shows the lower $g_\perp$ value.

Figure 6 shows the ENDOR spectra at $g_\parallel = 1.996$ and $g_\perp = 1.872$ of the Ti^{3+} ions in the amorphous solid of C_3H_7OH/H_2O. The ENDOR spectra at $g_\parallel = 2.000$ and $g_\perp = 1.778$ were too weak to be detected. Broad and weak ENDOR spectra by the coordinated H_2O molecules were observed on both sides of the intense distant matrix ENDOR spectra. The ENDOR spectra calculated from $\omega_{\alpha,\beta}$ in eq 3 with the geometrical parameters determined by the ESE experiment ($\zeta = 60°$, $R = 2.2$ Å, $\psi = 0°$, $\xi = 0°$ for $g_\parallel$ and $\xi = 90°$ for $g_\perp$) are also shown in Figure 6 with broken lines. The observed spectra were reproduced by using a Gaussian line shape $\exp(-\nu^2/w^2)$ with $w = 2$ MHz and the proton hyperfine coupling constants of 7 and 5 MHz for $g_\parallel$ and $g_\perp$, respectively. The coupling constants of 7 and 5 MHz correspond to the deuteron isotropic hyperfine coupling constants of 1.05 and 0.75 MHz, respectively. Although the coupling constants are slightly larger than those determined by the ESE experiment, probably because of the difference of the spectral positions between the ENDOR and the ESE measurements and because of the inaccuracy of the assumed line shape, they show the same tendency: the coupling constant for the hydrated ion with the $g_\perp$ value smaller than the average $g_\perp$ of 1.896 is smaller than the average coupling constant at the $g_\parallel$ position.

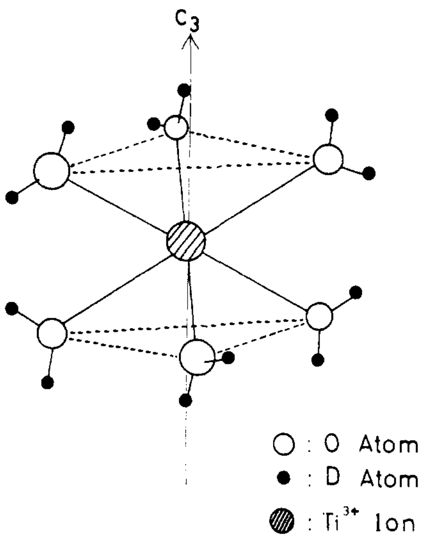

Figure 7. Hydration structure of the Ti^{3+} ion in the 2-propanol/D_2O mixture deduced from the analysis of ESE modulation signal. Six water molecules are coordinated to the central Ti^{3+} ion with D_{3d} symmetry. The Ti^{3+}–O bond bisects the D–O–D angle. The angle between the Ti^{3+}–O bond and the C_3 axis is 60°. The D_2O molecular plane is parallel to the C_3 axis.

Discussion

The hydration structure determined from the analysis of the ESE deuteron modulation is shown in Figure 7. In this structure, the metal ion is coordinated to six water molecules to form an octahedron with a slight compression along the C_3 axis. The hydrated ion possesses D_{3d} symmetry. The D–O–D plane is parallel to the C_3 axis. The Ti^{3+}–O distances and the angles between the C_3 axis and the Ti^{3+}–O bonds are 2.2 Å and 60°, respectively. The distance of 2.2 Å is slightly longer than the expected Ti^{3+}–O distance in the alum crystal (2.1 Å)[2] and the sum of the ionic radii of the Ti^{3+} ion (0.81 Å) and O^{2-} (1.26 Å).[15] This discrepancy might arise from the oversimplified assumption that the unpaired electron is located on the Ti nucleus. It is therefore safer to say that the distance is about 2.2 Å.

The axial symmetry of the ESR spectrum and the decrease of the hyperfine coupling constant with the decrease of the $g_\perp$ value can be explained by taking the interaction between the singly occupied d orbital of the Ti^{3+} ion and D_2O molecular orbitals. As is schematically shown in Figure 8, the degenerate d orbitals of the Ti^{3+} ion split into t_{2g} and e_g states under O_h symmetry. These states further split into a_{1g}, e_g, and e_g' states if there is an axial field. The axial field arises from the repulsive interaction between the a_{1g} orbital and the molecular orbitals of D_2O. The molecular orbitals able to interact with the Ti^{3+} ion are nonbonding n_σ, nonbonding n_π, and π_{OD_2}. The n_σ and the π_{OD_2} orbitals are parallel to the molecular plane whereas the n_π orbital is perpendicular to the molecular plane. The n_σ orbital makes a coordination bond. The strength of the coordination bond is maximum when the Ti^{3+}–O bond bisects the D–O–D angle. The molecular dipoles of the coordinated D_2O molecules are therefore aligned toward the central Ti^{3+} ions. The a_{1g} orbital repulsively interacts with the n_π and the π_{OD_2} orbital. Since the n_π orbital is closer to the Ti^{3+} ion than the π_{OD_2} orbital, the repulsive interaction with the n_π orbital is potentially much stronger than that with the π_{OD_2} orbital. The strength of these repulsive interactions depends on the angle of the D_2O molecular plane with respect to the a_{1g} orbital or the C_3 axis. The n_π orbital is orthogonal to the a_{1g} orbital if the molecule plane is parallel to the C_3 axis. Under this configuration the repulsive interaction with the n_π orbital is minimum and the weaker repulsive interaction with the π_{OD_2} orbital is maximum. The spin density at the deuterons is therefore maximum. On the other hand, if the molecular plane rotates 90° about the Ti^{3+}–O axis, the repulsive interaction with the n_π orbital becomes maximum and the spin density at the deuterons becomes minimum. The rotation of the D–O–D plane from the parallel position therefore causes the decrease of both the isotropic hyperfine coupling constant and the stability of the hydration structure.

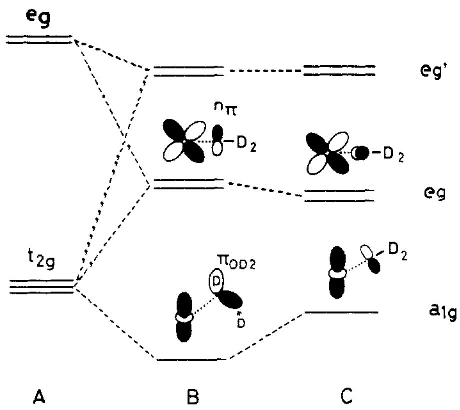

Figure 8. Schematic diagram showing the energy level of the hydrated Ti^{3+} ion and the repulsive orbital interactions between Ti^{3+} and the coordinating D_2O under (A) O_h symmetry with no orbital interaction except for repulsive electrostatic interactions, (B) D_{3d} symmetry with the D–O–D plane parallel to the C_3 axis, and (C) D_{3d} symmetry with the D–O–D plane perpendicular to the C_3 axis.

If the energy differences between the a_{1g} and the upper e_g and $e_{g'}$ orbitals are not so small, the g factors of the Ti^{3+} ion under the D_{3d} symmetry is roughly given by[16]

$$g_\parallel = 2.0023, \quad g_\perp = 2.0023(1 - 121/\Delta - 242/\Delta') \quad (10)$$

where Δ and Δ' denote the energy differences between a_{1g} and e_g and between a_{1g} and $e_{g'}$ orbitals, respectively. The value of Δ' is determined from the optical absorption spectrum of the hydrated ions to be 20 000 cm^{-1}. The $g_\perp$ factor of the hydrated ion is therefore mainly determined by the energy difference between the a_{1g} and the e_g orbitals. As is shown in Figure 8, the e_g orbital mainly interacts with the n_π orbital. The repulsive interaction between these orbitals is maximum when the D_2O molecular plane is parallel to the C_3 axis. Since the ground-state energy under this configuration is the lowest, the hydrated ion shows the largest $g_\perp$ factor and the largest isotropic hyperfine coupling constant. The repulsive interaction between the a_{1g} and the n_π orbitals is decreased by the rotation of the D–O–D plane about the Ti^{3+}–O axis and is minimum when the D–O–D plane is perpendicular to the C_3 axis. Since the rotation of the D–O–D plane causes the increase of the ground-state energy, it causes the decrease of the $g_\perp$ factor, the hyperfine coupling constant, and the stability of the hydration structure. The hydration structure of the Ti^{3+} ion observed at $g = 1.778$ must be different from that observed at $g_\parallel = 2.000$. However, the difference is too small to be detected by the ESE method.

Although the hydration structure of the Ti^{3+} ion in the alum crystal, $CsTi(SO_4)_2 \cdot 12H_2O$, is similar to that in the amorphous solid, the g factors ($g_\parallel = 1.25$, $g_\perp = 1.14$) are much different from those in the amorphous solid. This difference can be explained by taking the angle between the C_3 axis and the D–O–D plane. Although the detailed hydration structure in the alum crystal is not known, it is expected to be similar to that of Al^{3+} in a $CsAl(SO_4)_2 \cdot 12D_2O$ crystal.[2] In this crystal, an Al^{3+} ion is coordinated by six water molecules to form a regular octahedron. The coordinating D_2O is hydrogen bonded to a SO_4 oxygen and an oxygen of D_2O coordinating another Cs^+ ion. All the D–O–D planes are not parallel to the C_3 axis. Two of six D–O–D planes are almost perpendicular to the C_3 axis. The energies of the a_{1g} and the e_g orbitals of the Ti^{3+} ion in the alum crystal are therefore expected to be higher and lower than those of the Ti^{3+} ion in the amorphous solid, respectively. The g factors cannot be estimated

---

(15) Shannon, R. D. *Acta Crystallogr.* **1976**, *A32*, 751.

(16) Griffith, J. S. In *The Theory of Transition Metal Ions*; Cambridge University Press: London, 1961; p 437.

by eq 10 if the energy of the e_g orbital is close to that of the a_{1g} orbital and they are much smaller than 2.0023. The hydrated ion in the alum crystal therefore shows small *g* factors. Although the energy of the a_{1g} orbital is higher, this hydration structure is stable in the crystal because the increase of the orbital energy is compensated by the strong hydrogen bondings between the coordinating water and the surrounding water molecules and ions. The distortion of the hydration structure is concluded to arise from the long-range order of the crystal structure.

Acknowledgment. We thank Professor A. Lund at the Linköping Institute of technology for measuring the ENDOR spectrum of the hydrated Ti^{3+} ion.

Registry No. Ti, 22541-75-9; C_3H_7OH, 67-63-0; D_2O, 7789-20-0.

Geometrical Structure and Electronic States of the Hydrated Titanium(III) Ion. An ab Initio CI Study

Hiroto Tachikawa, Tsuneki Ichikawa,* and Hiroshi Yoshida

Contribution from the Faculty of Engineering, Hokkaido University, Sapporo 060, Japan.

Received May 2, 1989

Abstract: The geometrical structure and the electronic states of the hydrated Ti^{3+} ion, $[Ti(H_2O)_6]^{3+}$ complex, have been studied by means of ab initio MO calculations including electron correlation. The optimized geometrical structure is in good agreement with the structure that has been experimentally determined by means of an electron spin-echo modulation analysis. The complex possesses D_{3d} symmetry, which is slightly distorted from O_h symmetry by the Jahn-Teller effect. The electronic ground state is the $^2A_{1g}$ state in which the unpaired electron is mainly distributed in the d_{z^2} orbital. The g tensor of $g_\parallel = 2.000$ and $g_\perp = 1.864$ calculated by a second-order perturbation method with the wave functions obtained from the MR-SD-CI calculation is in good agreement with the experimental values. The shoulder of the electronic absorption spectrum appearing at 570 nm is determined to be caused by the Jahn-Teller distortion of the excited $^2E_g'$ state.

Since hydration of metal ions plays an important role in structural chemistry and chemical reactions in aqueous solutions, it has been extensively studied experimentally[1-3] and theoretically.[4-6] The hydrated trivalent titanium ion, $[Ti(H_2O)_6]^{3+}$ complex, is one of the simplest paramagnetic transition-metal complexes that has only one electron in the d orbital. However, the structure of the $[Ti(H_2O)_6]^{3+}$ complex has not been much studied because of its chemical instability. The structure of the $[Ti(H_2O)_6]^{3+}$ complex in the crystal of cesium titanium alum, $CsTi(SO_4)_2 \cdot 12H_2O$, has been studied by using electron spin resonance (ESR),[7] UV, and visible spectroscopies.[8] It has been concluded from these studies that the $[Ti(H_2O)_6]^{3+}$ complex in the alum crystal has C_3 symmetry with the water molecules aligned toward the central Ti^{3+} ion. However, the hydration structure of the Ti^{3+} ion in water is not the same as that in the alum, because the ESR spectrum of the Ti^{3+} ion in glassy water is totally different from that in the alum crystal.

The hydrated Ti^{3+} ion in water shows a characteristic absorption spectrum around 500 nm with the shoulder at 570 nm.[9] Three structural models have been proposed for explaining the absorption spectrum; The first model[10] is based on the crystal field (CF) theory[11] and assumes O_h symmetry as a starting structure. The d orbitals then split into the t_{2g} and e_g orbitals. Owing to electrostatic interactions, the unpaired electron in the d_{xy} orbital pushes the four ligands on the *xy* plane away from the central metal ion. The symmetry is therefore changed from O_h to D_{2h}, and an absorption band due to the $^2T_{2g}$ to ^2E_g transition emerges in the visible region. The second model[12] was proposed for explaining the shoulder band at 570 nm. The ground state in this model is assumed to have O_h symmetry. The excited ^2E_g state splits into the $^2A_{1g}$ and $^2B_{1g}$ states because of the Jahn-Teller effect. The absorption bands at 500 and 570 nm are therefore assigned to be $^2T_{2g}$ to $^2B_{1g}$ and $^2T_{2g}$ to $^2A_{1g}$ transitions, respectively. The third model[13] assumes the structure to be a distorted octahedron (D_{3d} symmetry) with compression along the C_3 axis. The orbitals generated by mixing of the d orbitals are a_{1g}, e_g, and e_g'. The absorption bands are assigned to be the transition from a_{1g} to e_g (500 nm) and to e_g' (570 nm), respectively.

We have studied the geometrical structure of the $[Ti(D_2O)_6]^{3+}$ complex in the amorphous solid of a 2-propanol/D_2O mixture by means of ESR and electron spin-echo (ESE) techniques and concluded that the complex is in D_{3d} symmetry with the $g_\parallel$ and $g_\perp$ factors of 1.994 and 1.896, respectively.[14] The optical absorption spectrum of the complex in the amorphous solid is the same as that of the hydrated Ti^{3+} ion in the aqueous solution, so that the determined structure is the same as the hydration structure of the Ti^{3+} ion in water.

In the present study, ab initio molecular orbital calculations including electronic correlation have been performed on the $[Ti(H_2O)_6]^{3+}$ complex. The main purposes of this study are (1)

---

(1) Ichikawa, T.; Yoshida, H.; Li, A. S. W.; Kevan, L. *J. Phys. Chem.* **1984**, *106*, 4324.

(2) Ichikawa, T.; Kevan, L. *J. Phys. Chem.* **1980**, *84*, 1955.

(3) Ichikawa, T.; Kevan, L.; Narayana, P. A. *J. Chem. Phys.* **1979**, *71*, 3793.

(4) Blair, J. T.; Westbrook, J. D.; Levy, R. M.; K-Jecpersen, K. *Chem. Phys. Lett.* **1989**, *154*, 531.

(5) Dhar, S.; Kestner, N. R.*Radiat. Phys. Chem.* **1988**, *32*, 355.

(6) Arbman, M.; Siegbahn, H.; Pettersson, L.; Siegbahn, P. *Mol. Phys.* **1985**, *54*, 1149.

(7) Bijl, D. *Proc. Phys. Soc.* (*London*) **1950**, *A63*, 405.

(8) Holmes, O. G.; McClure, D. S. *J. Chem. Phys.* **1957**, *26*, 1686.

(9) Cottn, F. A. *J. Chem. Educ.* **1964**, *41*, 446.

(10) Basolo, F.; Johnson, R. *Coordination Chemistry*; W. A. Benjamin, Inc.: New York, 1964.

(11) Sutton, L. E. *J. Chem. Educ.* **1960**, *37*, 498.

(12) Murrel, J. N.; Kettle, S. F. A.; Tedder, J. M. *Valence Theory*, 2nd ed.; John Wiley & Sons Inc: London, 1965.

(13) Jarrett, H. S. *J. Chem. Phys.* **1957**, *27*, 1298.

(14) Tachikawa, H.; Ichikawa, T.; Yoshida, H. *J. Am. Chem. Soc.*, preceding paper in this issue.

0002-7863/90/1512-982$02.50/0